BPSK based Subcarrier Intensity Modulated Free Space Optical System in Combined Strong Atmospheric Turbulence

Prabu K, Sumanta Bose, D. Sriram Kumar
Department of Electronics and Communication Engineering
National Institute of Technology, Tiruchirappalli.
India

ABSTRACT- In this paper the performance of a Free Space Optical (FSO) communication system is analyzed by considering heavy atmospheric losses such as scattering, absorption, channel fading and misalignment fading. For the analysis, subcarrier intensity modulated free space optical (SIM-FSO) communication system using binary phase shift keying (BPSK) is employed. The Bit Error Rate (BER), channel capacity and outage probability of the radiated signal is then investigated over a K-distributed mutual slow fading turbulence channel with illustrative 2D and 3D plots. Novel closed-form analytical expressions are derived for the strong turbulent channel model, average BER, channel capacity and outage probability for the considered communication system.

Key words – Free space optics, Bit error rate, Channel capacity, Outage probability, Sub carrier intensity modulation.

1. Introduction

Free space optical (FSO) communication, a form of high speed wireless optical communication relies on pure line of sight (LOS) technology. Its performance strongly depends on the atmospheric conditions between the transmitter and receiver [1,2]. The foremost advantages of wireless optical communications are high bandwidth, high security and ease installation without license [3]. The key applications FSO communication includes inter and intra chip communication [4,5], inter satellite communication [6,7], alternative technology for optical fiber networks [8], temporary network installation [9] and radio over FSO communications [10]. However, the major drawback of FSO is natural turbulence

[11]. To improve the signal quality in the receiver side various channel models, modulation techniques and diversity techniques are used [16, 25]. In general, the wireless channel is modeled as Gamma-gamma [12,13], Rayleigh[14] or Exponential channel model [15,16] among others. The performance of the FSO system is generally analyzed by computing the bit error rate (BER), outage probability and channel capacity [17, 18].

In a recent work, [19], the optical channel has been systematically described using a mutual slow fading channel model. Its performance analysis parameters such as outage probability, channel capacity and the link impairments imposed by the atmospheric attenuation due to beam extinction were also evaluated. They also investigated the channel fading due to turbulence and pointing errors for an on-off keying FSO system. In another work, [20], the performance of a sub carrier intensity modulated free space optical (SIM-FSO) communication system was investigated over a K-distributed turbulence channel.

In this paper, the performance of SIM-FSO communication system using binary phase shift keying (BPSK) is investigated over a K-distributed mutual slow fading turbulence channel. Novel equations are derived for BER, outage probability and channel capacity for the considered system. The performance analysis and results are illustrated through 2D and 3D plots.

The paper is organized as follows: Section 2 discusses the SIM-FSO system model used in our work. In Section 3, the mutual channel fading model is discussed. In Section 4, expressions for average BER, channel capacity and outage probability for the considered system are derived and presented. Section 5 describes the numerical results with graphical analysis. Finally, concluding remarks are highlighted in Section 6.

2. BPSK based SIM-FSO communication system

The considered BPSK based SIM-FSO system with K-distributed turbulence channels is represented in Fig. 1. BPSK based subcarrier intensity modulated signal is transmitted through the channel, along with additive white Gaussian noise in the presence of beam extinction and pointing errors. In Fig. 1, the

transmitted signal is scattered due to natural turbulence in the atmospheric channel (AC). These turbulences are caused by rain, fog, smoke, smog, heavy dust particles, etc. But heavy fog, as shown in Fig. 1, causes the maximum attenuation in the transmitted signal. In this work we consider strong atmospheric turbulence condition for the analysis of the FSO system. The scattered components and the LOS component are clearly shown in the figure. At the receiver, the signal(y) is detected via a finite Gaussian lens [21], expressed as:

$$y = h\gamma P_{FSO} x + n \tag{1}$$

where h is the channel state, γ is the detector responsivity, x is the transmitted signal, n is the noise caused by various sources and P_{FSO} is the average optical transmitted power. The channel state h models the optical intensity fluctuations [2] resulting from atmospheric loss, turbulence and fading as:

$$h = h_l h_s h_p \tag{2}$$

where h_l is the attenuation due to beam extinction and path loss, h_s due to scintillation effects and h_p due to the geometric spread and pointing errors.
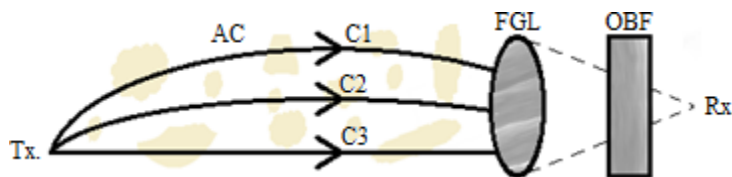
AC: Atmospheric channel
OBF: Optical bandpass filter
FGL: Finite Gaussian lens

C1: Independent scatter component
C2: Coupled to LOS component
C3: Line of sight (LOS) component

Fig. 1. Block diagram of communication system with k-distributed turbulence channels

The received electrical signal to noise ratio as considered in [22] is expressed as:

$$SNR(h) = \frac{(\gamma h)^2}{2\sigma_n^2} \tag{3}$$

where σ_n^2 is the variance of the channel noise.

3. Channel models of FSO systems

The combined channel fading model that has been presented in [19] is derived with the combination of atmospheric turbulence induced fading and misalignment fading for both weak and strong atmospheric turbulence conditions.

For weak atmospheric turbulence conditions, the channel model expressed as the probability density function of the irradiance intensity, h as given by [19] is:

$$f_h(h) = \frac{\xi^2}{(A_0 h_l)^{\xi^2}} h^{\xi^2-1} \times \int_{h/A_0 h_l}^{\infty} \frac{1}{h_s^{\xi^2+1} \sigma_I(D)\sqrt{2\pi}} \exp\left(-\frac{[\ln(h_s)+0.5\,\sigma_I^2(D)]^2}{2\sigma_I^2(D)}\right) dh_s \qquad (4)$$

where $\sigma_I^2(D)$ is the aperture averaged scintillation index, $\xi = w_{z_{eq}}/\sigma_s$ is the ratio between the equivalent beam radius at the receiver and the pointing error displacement standard deviation at the receiver and A_0 is the fraction of the received power at zero radial distance.

For strong atmospheric turbulence conditions, the channel model expressed as the probability density function of the irradiance intensity, h as given by [19] is:

$$f_h(h) = \frac{2\xi^2(\alpha\beta)^{(\alpha+\beta)/2}}{(A_0 h_l)^{\xi^2}\Gamma(\alpha)\Gamma(\beta)} h^{\xi^2-1} \times \int_{h/A_0 h_l}^{\infty} h_s^{(\alpha+\beta)/2-1-\xi^2} K_{(\alpha-\beta)}\left(2\sqrt{\alpha\beta h_s}\right) dh_s \qquad (5)$$

where α and β are the effective number of large and small scale turbulent eddies, $\Gamma(\cdot)$ is the gamma function. $K_{(\alpha-\beta)}$ is the modified Bessel function of the second kind of order $(\alpha-\beta)$ which can be simplified using Meijer G function [23, Eq. (14)]. Then using [24, Eq.(07.34.21.0085.01)], a closed-form expression for the channel model is obtained, as proved in Appendix A and expressed by Eq. (6).

$$f_h(h) = \frac{\alpha\beta\xi^2}{A_0 h_l \Gamma(\alpha)\Gamma(\beta)} G_{1,3}^{3,0}\left[\frac{\alpha\beta h}{A_0 h_l}\bigg|_{-1+\xi^2,\alpha-1,\beta-1}^{\xi^2}\right] \qquad (6)$$

4. Performance analysis of proposed BPSK based SIM-FSO system

The performance of the considered system is evaluated on the basis of average BER, channel capacity and outage probability.

4.1. Bit error rate

In the considered SIM-FSO communication system, the subcarrier is pre-modulated using BPSK. By modulating the optical signal with radio frequency, the subcarrier provides SIM. For a coherent BPSK demodulator, the probability of conditional BER depending on the intensity fluctuation [25,26] is expressed as:

$$P_{e/h}(h) = Q\left(\frac{h\gamma}{\sqrt{2}\sigma_n}\right) = 0.5 \times \text{erfc}\left(\frac{h\gamma}{2\sigma_n}\right) \tag{7}$$

where γ is the photo detector responsivity, σ_n^2 is the variance of the channel noise and $Q(\cdot)$ is the Gaussian Q function related to the complementary error function $\text{erfc}(\cdot)$ as $2Q(\sqrt{2}x) = \text{erfc}(x)$.

The probability of average BER for BPSK based SIM-FSO over K-distributed mutual slow fading turbulence channel can be achieved by using Eq. (8).

$$P_e = \int_0^\infty P_{e/h}(h) f_h(h)dh \tag{8}$$

By using Eq. (6) and (7) in (8), we get:

$$P_e = \frac{\alpha\beta\xi^2}{A_0 h_l \Gamma(\alpha)\Gamma(\beta)} \times \int_0^\infty 0.5 \, \text{erfc}\left(\frac{h\gamma}{2\sigma_n}\right) \times G_{1,3}^{3,0}\left[\frac{\alpha\beta h}{A_0 h_l}\middle|\begin{matrix}\xi^2\\-1+\xi^2,\alpha-1,\beta-1\end{matrix}\right]dh \tag{9}$$

By expressing the $\text{erfc}(\cdot)$ as Meijer G function [27, Eq. (8.4.14.2)], the probability of average BER can be expressed in a closed-form by utilizing [23, Eq. (21)]. As proved in Appendix B, this integration can be simplified to obtain:

$$P_e = \frac{2^{\alpha+\beta-4}\xi^2}{\sqrt{\pi^3}\Gamma(\alpha)\Gamma(\beta)} G_{7,4}^{2,6}\left[\frac{4\gamma^2 A_0^2 h_l^2}{\sigma_n^2\alpha^2\beta^2}\middle|\begin{matrix}\frac{1-\xi^2}{2},\frac{2-\xi^2}{2},\frac{1-\alpha}{2},\frac{2-\alpha}{2},\frac{1-\beta}{2},\frac{2-\beta}{2},1\\0,\frac{1}{2},\frac{-\xi^2}{2},\frac{-\xi^2+1}{2}\end{matrix}\right] \tag{10}$$

4.2. Channel capacity

The channel capacity is a quantitative measurement of the limiting data transmission rate that can be achieved through a non-deterministic fading channel with minimum probability of error. For a BPSK based SIM-FSO channel it can be estimated using mathematical analogy from [28] as follows:

$$\langle C \rangle = \int_0^\infty B \times \log_2\left(1 + \frac{(\gamma h)^2}{2\sigma_n^2}\right) f_h(h)dh \tag{11}$$

where B is the signal transmission bandwidth.

By expressing the logarithm function as the Meijer G function [23, Eq. (11)], Eq. (11)is simplified to obtain a closed-form mathematical expression for the channel capacity expressed as Eq. (12). The proof is available in Appendix C.

$$\langle C \rangle = B \times \frac{2^{\alpha+\beta-4}A_0 h_l}{\pi\alpha\beta\cdot\ln(2)} G_{8,4}^{1,8}\left[\frac{8\gamma^2 A_0^2 h_l^2}{\sigma_n^2 \alpha^2 \beta^2}\Bigg|^{1,1,\frac{1-\xi^2}{2},\frac{2-\xi^2}{2},\frac{1-\alpha}{2},\frac{2-\alpha}{2},\frac{1-\beta}{2},\frac{2-\beta}{2}}_{\qquad\quad 1,\frac{-\xi^2}{2},\frac{-\xi^2+1}{2},0}\right] \tag{12}$$

4.3. Outage probability

In a slow fading channel model the amplitude and phase change forced by the channel is approximately constant over time. The outage probability of a BPSK based SIM-FSO system over slow fading channel [17] is expressed as:

$$P_{out} = P(SNR(h) \leq SNR_{th}) \tag{13}$$

where SNR_{th} is the threshold SNR value below which the signal strength at the receiver side is less than acceptable limits. Further simplifying by using Eq. (3), we get:

$$P_{out} = P\left(h \leq \sqrt{\frac{2\sigma_n^2 \cdot SNR_{th}}{\gamma^2}}\right) = F_I\left(\sqrt{\frac{2\sigma_n^2 \cdot SNR_{th}}{\gamma^2}}\right) \tag{14}$$

where $F_I(\cdot)$ is the cumulative distribution function (CDF) of the K-distributed random variable. The CDF of h is derived using [27, Eq. (2.24.2.2)] as:

$$P_{out} = \frac{1}{\Gamma(\alpha)\Gamma(\beta)} G_{1,3}^{2,1}\left[\alpha\beta\sqrt{\frac{2\sigma_n^2 \cdot SNR_{th}}{\gamma^2}}\Bigg|^{1}_{\alpha,\beta,0}\right] \tag{15}$$

To the best of the author's knowledge, the expressions for strong turbulent channel model (Eq. (6)), average BER (Eq. (10)), channel capacity (Eq. (12)) and outage probability (Eq. (15)) are new to the analysis of the performance of BPSK based SIM-FSO system.

5. Numerical results and discussions

For the purpose of numerical evaluation, the proposed BPSK based SIM-FSO system is considered having noise standard deviation $\sigma_n = 10^{-7}$ A/Hz, photo detector responsivity $\gamma = 0.5$ A/W, beam radius $w_L \cong 2.5$ m at 1 km distance and jitter standard deviation $\sigma_s \cong 30$ cm. Fig. 2 illustrates the average BER performance of the SIM-FSO system in terms of responsivity for different values of the effective number of large scale (α) and small scale (β) turbulent eddies.

It is observed that better BER performance is achieved by using high responsivity detector in the receiver. Among the considered cases, we obtained the best BER performance for $\alpha = 7$ and $\beta = 3$. This is because α accounts for large scale turbulent eddies and larger value of α implies lesser atmospheric turbulences. Larger value of β also implies lesser atmospheric turbulences but its impact is weaker compared to α, since β only accounts for small scale turbulent eddies.
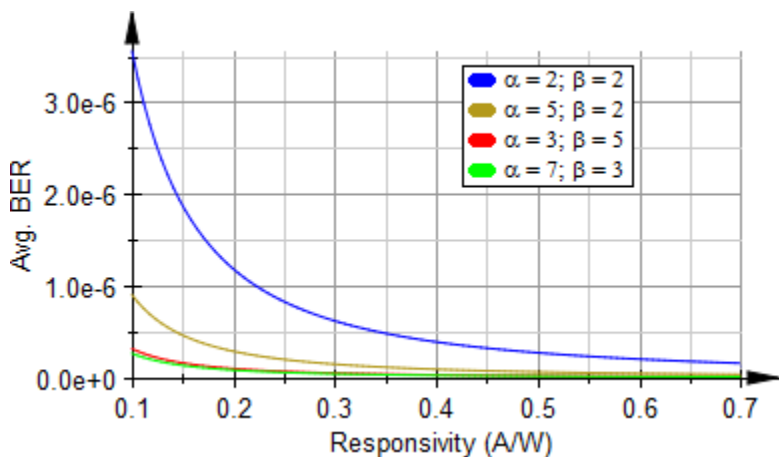

Fig. 2. BER variation with respect to the responsivity of the photo detector

Fig. 3 shows the BER performance of the BPSKbased SIM-FSO system evaluated against the average SNR for different values of α and β. As the SNR increases the average BER decreases as expected. It is known that the decrement pattern of average BER with respect to SNR is concave outward i.e. rapid decrement in cases of clear weather [20]. However, in our case of heavy atmospheric turbulence, the average BER decrement is gradual (concave inward as in Fig. 3) with increasing SNR even beyond 20dB. This is due to the disturbances in the atmosperic channel caused by heavy fog, etc.
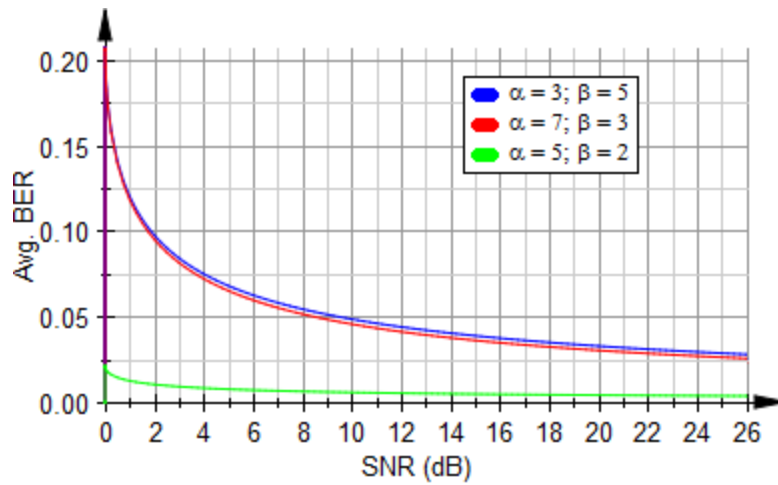
Fig. 3. BER against average SNR for various values of the parameter α and β

The 3D plots shown in Fig. 4 depict the trade-off between the average BER against the effective number of large scale (α) and small scale (β) turbulent eddies. From Fig. 4 it is observed that the BER of BPSK based SIM-FSO system decreases as the values of α and β increases. This is because larger value of α and β implies lesser atmospheric turbulences. α and β increases till 10 each in Fig. 4(a), 11 each in Fig. 4(b) and 13 each in Fig. 4(c). It is also observed that as α and β increases beyond 10, the BER increases abruptly.

(a)

(b)
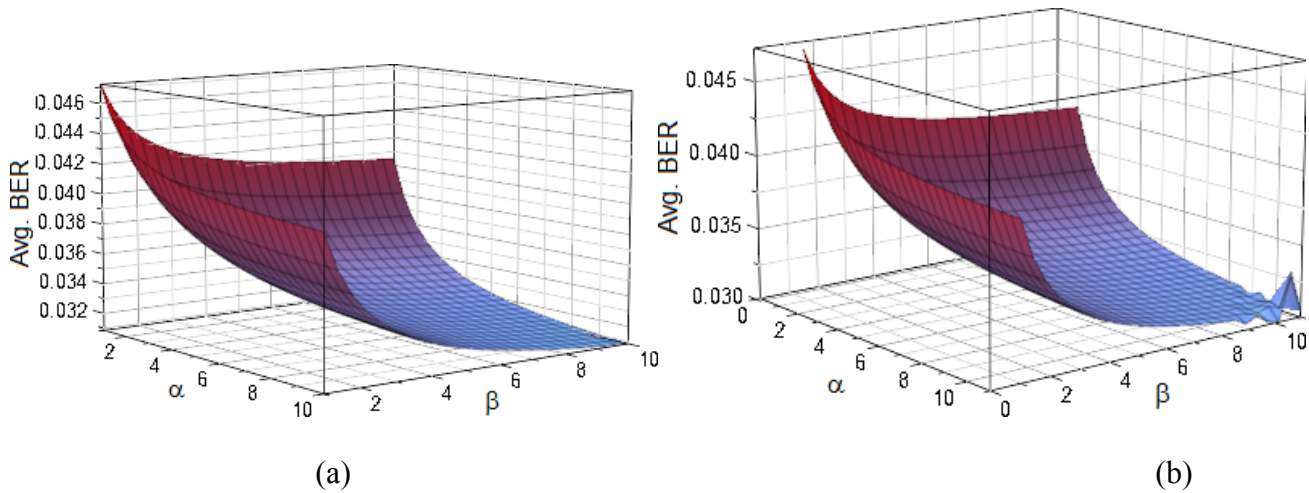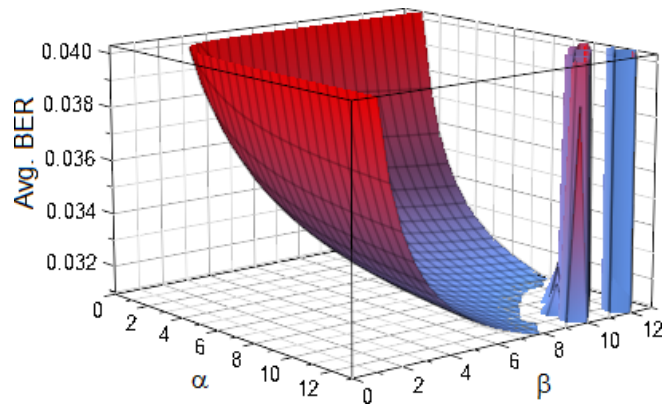
(c)

Fig. 4.3D plot for BER variation with respect to α and β

Fig. 5 shows the channel capacity against the average SNR under strong turbulence atmospheric channel. It is observed from Fig. 3 and Fig. 5 that a larger value of SNR implies a lesser BER and a greater channel capacity.
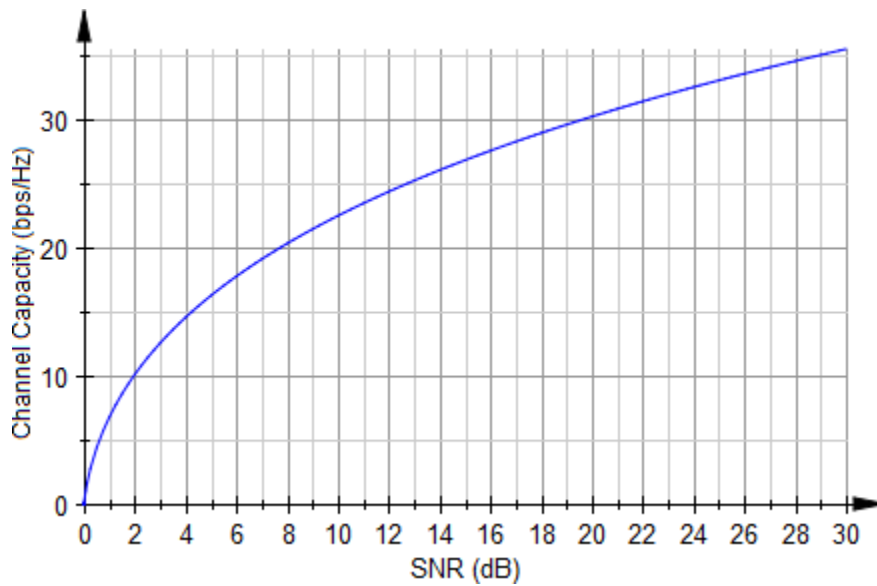

Fig. 5. Channel capacity versus SNR

Fig. 6 presents the outage probability in terms of the threshold achievable rate under strong turbulence condition. It is observed that a lesser threshold SNR (SNR_{th}) causes the receiver to pick up relatively weaker signals, thus decreasing the probability of signal outage at the receiver.
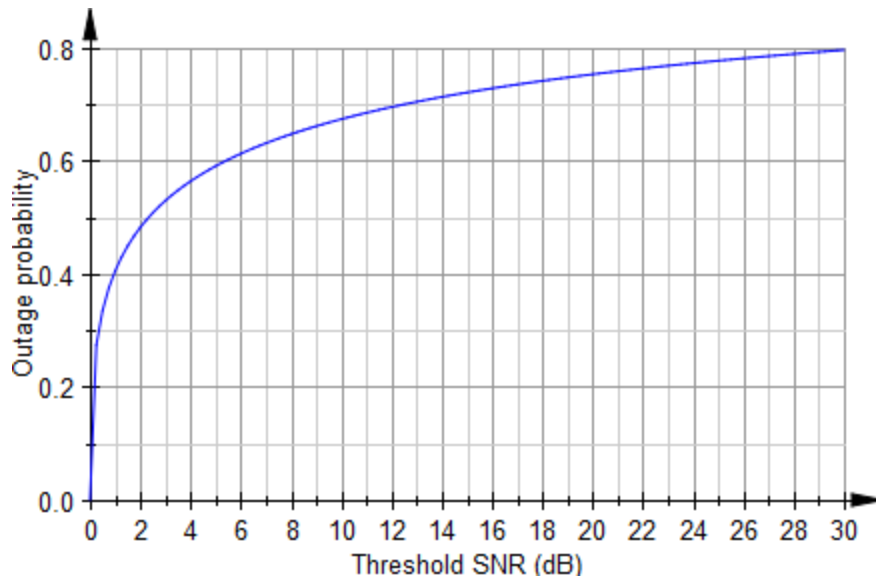
Fig. 6. Outage probability versus threshold SNR

6. Conclusion

A BPSK based SIM-FSO channel weakened by strong atmospheric attenuation and channel fading was studied. The primary cause causing the turbulence and pointing error was identified as heavy fog. Mathematical expressions for the combined channel fading model (induced fading and misalignment fading) were derived. A BPSK signal was transmitted through the considered SIM-FSO system operating over K-distributed channels in the presence of strong atmospheric turbulence. The performance of the system was analyzed by deriving novel closed-form analytical expressions for average BER, channel capacity and outage probability of the system. It was observed that better BER performance could be obtained by increasing the detector responsivity or increasing the SNR. Also, an atmospheric system having lesser atmospheric turbulences (i.e. higher value of effective large and small scale turbulent eddies) was observed to exhibit better BER performance. A transmission with higher SNR was observed to provide greater channel capacity. It was also observed that a detector having lower threshold SNR value could pick up relatively weaker signals thus reducing the outage probability.

Appendix: A: Proof of channel model [Eq. (6)]

The channel model of our considered SIM-FSO system is reproduced from Eq. (5).

$$f_h(h) = \frac{2\xi^2(\alpha\beta)^{(\alpha+\beta)/2}}{(A_0 h_l)^{\xi^2}\Gamma(\alpha)\Gamma(\beta)} h^{\xi^2-1} \times \int_{h/A_0 h_l}^{\infty} h_s^{(\alpha+\beta)/2-1-\xi^2} K_{(\alpha-\beta)}\left(2\sqrt{\alpha\beta h_s}\right) dh_s \tag{A.1}$$

The Bessel function $K_v(x)$ of the second kind having order v can be expressed as Meijer G function using Eq. (A.2). Using this identity, Eq. (A.1) reduces to Eq. (A.3).

$$K_v(x) = \frac{1}{2} G_{0,2}^{2,0}\left[\frac{x^2}{4}\middle|\begin{matrix} - & - \\ v/2 & -v/2 \end{matrix}\right] \tag{A.2}$$

$$f_h(h) = \frac{2\xi^2(\alpha\beta)^{(\alpha+\beta)/2}}{(A_0 h_l)^{\xi^2}\Gamma(\alpha)\Gamma(\beta)} h^{\xi^2-1} \times \frac{1}{2} \times \int_{h/A_0 h_l}^{\infty} h_s^{(\alpha+\beta)/2-1-\xi^2} G_{0,2}^{2,0}\left[\alpha\beta h_s\middle|\begin{matrix} - & - \\ (\alpha-\beta)/2 & (\beta-\alpha)/2 \end{matrix}\right] dh_s \tag{A.3}$$

Then [24, Eq. (07.34.21.0085.01)] is used to solve the above integral followed by further simplification using [24, Eq. (07.34.16.0001.01)] to obtain Eq. (6).

Appendix: B: Proof of average BER [Eq. (10)]

The probability of average BER expressed by Eq. (9) is reproduced.

$$P_e = \frac{\alpha\beta\xi^2}{A_0 h_l \Gamma(\alpha)\Gamma(\beta)} \times \int_0^{\infty} 0.5\ \text{erfc}\left(\frac{h\gamma}{2\sigma_n}\right) \times G_{1,3}^{3,0}\left[\frac{\alpha\beta h}{A_0 h_l}\middle|\begin{matrix} \xi^2 \\ -1+\xi^2, \alpha-1, \beta-1 \end{matrix}\right] dh \tag{B.1}$$

The complementary error function erfc($\cdot$) can be expressed as Meijer G function using Eq. (B.2). Using this identity, Eq. (B.1) reduces to Eq. (B.3).

$$\text{erfc}(\sqrt{x}) = \frac{1}{\sqrt{\pi}} G_{1,2}^{2,0}\left[x\middle|\begin{matrix} 1 \\ 0, 1/2 \end{matrix}\right] \tag{B.2}$$

$$P_e = \frac{\alpha\beta\xi^2}{A_0 h_l \Gamma(\alpha)\Gamma(\beta)} \times \int_0^{\infty} \frac{1}{2\sqrt{\pi}} G_{1,2}^{2,0}\left[\frac{\gamma^2 h^2}{4\sigma_n^2}\middle|\begin{matrix} 1 \\ 0, 1/2 \end{matrix}\right] \times G_{1,3}^{3,0}\left[\frac{\alpha\beta h}{A_0 h_l}\middle|\begin{matrix} \xi^2 \\ -1+\xi^2, \alpha-1, \beta-1 \end{matrix}\right] dh \tag{B.3}$$

By using [23, Eq. (21)] we solve the integral in Eq. (B.3) to obtain Eq. (10).

Appendix: C: Proof of channel capacity [Eq. (12)]

The channel capacity expressed by Eq. (11) is reproduced.

$$\langle C \rangle = \int_0^{\infty} B \times \log_2\left(1 + \frac{(\gamma h)^2}{2\sigma_n^2}\right) f_h(h) dh \tag{C.1}$$

By converting base of logarithm to e and using Eq. (6) for channel model, Eq. (C.1) reduces to Eq. (C.2)

$$\langle C \rangle = \frac{B}{\ln(2)} \times \frac{\alpha\beta\xi^2}{A_0 h_l \Gamma(\alpha)\Gamma(\beta)} \times \int_0^{\infty} G_{1,3}^{3,0}\left[\frac{\alpha\beta h}{A_0 h_l}\middle|\begin{matrix} \xi^2 \\ -1+\xi^2, \alpha-1, \beta-1 \end{matrix}\right] \times \ln\left(1 + \frac{(\gamma h)^2}{2\sigma_n^2}\right) dh \tag{C.2}$$

Any logarithmic function of the form $\ln(1 + x)$ can be expressed as Meijer G function using Eq. (C.3).

Using this identity, Eq. (C.2) reduces to Eq. (C.4).

$$\ln(1 + x) = G_{2,2}^{1,2}\left[x\Big|_{1,0}^{1,1}\right] \tag{C.3}$$

$$\langle C \rangle = \frac{B}{\ln(2)} \times \frac{\alpha\beta\xi^2}{A_0 h_l \Gamma(\alpha)\Gamma(\beta)} \times \int_0^\infty G_{1,3}^{3,0}\left[\frac{\alpha\beta h}{A_0 h_l}\Big|_{-1+\xi^2,\alpha-1,\beta-1}^{\xi^2}\right] \times G_{2,2}^{1,2}\left[\frac{(\gamma h)^2}{2\sigma_n^2}\Big|_{1,0}^{1,1}\right] dh \tag{C.4}$$

By using [23, Eq. (21)] we solve the integral in Eq. (C.4) to obtain Eq. (12).

References

[1] A.K. Majumdar, Free-space laser communication performance in the atmospheric channel, J. Opt. Fiber Commun. Res. 2 (2005) 345–396.

[2] A.A. Farid, S. Hranilovic, Outage capacity optimization for free-space optical links with pointing errors, J. Lightwave Technol. 25 (7) (2007) 1702–1710.

[3] W.O. Popoola, Z. Ghassemlooy, C.G. Lee, A.C. Boucouvalas, Scintillation effect on intensity modulated laser communication systems—a laboratory demonstration, Opt. Laser Technol. 42 (4) (2010) 682–692.

[4] Hui Wu, Berkehan Ciftcioglu and Rebecca Berman, Chip-scale demonstration of 3-D integrated intra-chip free-space optical interconnect, Proc. of SPIE. 8265 (2012).

[5] Tian Gu; Nair, R.; Haney, M.W., Integrated free-space optical interconnects: All optical communications on- and off-chip, Optical Interconnects Conference, 2012 IEEE , 74-75, 20-23 May 2012.

[6] Xin Li, Jing Ma, Siyuan Yu, Liying Tan, Tao Shen, Optimum signal input distribution design in the presence of random pointing jitter for inter-satellite optical communications, Optics &LaserTechnology45(2013)705–707.

[7] Vishal Sharma, Naresh Kumar, improved analysis of 2.5 Gbps-inter-satellite links (ISL) in inter-satellite optical-wireless communication (IsOWC) system, Optics Communications 286 (2013) 99–102.

[8] F. Xinghu, C. Zhenyi, G. Qiang, P. Fufei, W. Tingyun, Beam reception and data transmission performance analysis of optical taper used in a mobile wireless optical communication, Optik 122 (2011) 1646–1649.

[9] D. Keddar, S. Arnon, Urban optical wireless communication networks: The main challenges and possible solutions, IEEE Opt. Commun. (2004) S1–S7.

[10] Prabu, K; Bose, Sumanta; Sriram Kumar, D.;, "Analysis of optical modulators for Radio over Free Space Optical Communication systems and Radio over Fiber systems, India Conference (INDICON), 2012 Annual IEEE , vol., no., pp.1176-1179, 7-9 Dec. 2012, doi: 10.1109/INDCON.2012.6420795

[11] H.E. Nistazakis, T.A. Tsiftsis, G.S. Tombras, Performance analysis of free-space optical communication systems over atmospheric turbulence channels, IET Commun. 3 (2009) 1402–1409.

[12] Theodoros A., Tsiftsis,Harilaos G. Sandalidis, George K. Karagiannidis and Murat Uysal, Optical Wireless Links with Spatial Diversity over Strong Atmospheric Turbulence Channels, IEEE Transactions on Wireless Communications, 8 (2009) 951-957.

[13] T.A. Tsiftsis, Performance of heterodyne wireless optical communication systems over gamma-gamma atmospheric turbulence channels, Electronics Letters. 44 (2008).

[14] S.G.Wilson, Maïté Brandt-Pearce, Qianling Cao, Free-Space Optical MIMO Transmission With Q-ary PPM, Free-Space Optical MIMO Transmission With Q-array PPM, IEEE Transactions On Communications, 53 (8) (2005) 1402-1412.

[15] H.E. Nistazakisa, V.D. Assimakopoulosb, G.S. Tombrasa, Performance estimation of free space optical links over negative exponential atmospheric turbulence channels, Optik 122 (2011) 2191–2194

[16] Hector E. Nistazakis, A time-diversity scheme for wireless optical links over exponentially modeled turbulence channels, Optik - International Journal for Light and Electron Optics, Available online 2 July 2012.

[17] C. Liu, Y. Yao, Y. Sun and X. Zhao, Average capacity for heterodyne FSO communication systems over gamma-gamma turbulence channels with pointing errors, Electronics Letters. 46 (2010) 12.

[18] H.G.Sandalidis and T.A.Tsiftsis, Outage probability and ergodic capacity of free-space optical links over strong turbulence, Electronics Letters.44 (2008) 1.

[19] I.E.Lee, Z. Ghassemlooy, W. P. Ng, and M. Uysal, Performance Analysis of Free Space Optical Links over Turbulence and Misalignment Induced Fading Channels, 8th IEEE/IET International Symposium on Communication Systems, Networks & Digital Signal Processing (CSNDSP), (2012)1-6.

[20] Hossein Samimi, Optical Communication Using Subcarrier Intensity Modulation Through Generalized Turbulence Channels, Journal of Optical Communications and Networking, IEEE/OSA., 4 (5) (2012) 378-381.

[21] X.M.Zhu and J.M.Kahn, Free-space optical communication through atmospheric turbulence channels, IEEE Trans. Commun., 50(8) (2002) 1293-1300.

[22] H. Samimi and P. Azmi, Subcarrier intensity modulated free-space optical communications in K-distributed turbulence channels, J. Opt. Commun. Netw.,2 (8) (2010) 625–632.

[23] V. S. Adamchikand, O. I. Marichev, The algorithm for calculating integrals of hypergeometric type functions and its realization in REDUCE system, in Proc. Int. Conf. on Symbolic and Algebraic Computation, Tokyo, Japan. (1990) 212–224.

[24] Wolfram. (2001) The Wolfram functions site. Internet.[Online]. Available: http://functions.wolfram.com

[25] W. O. Popoola, Z. Ghassemlooy, J. I. H. Allen, E. Leitgeb, and S. Gao, Free-space optical communication employing subcarrier modulation and spatial diversity in atmospheric turbulence channel, IET Optoelectron., 2 (1) (2008) 16–23.

[26] W. O. Popoola and Z. Ghassemlooy, BPSK subcarrier modulated free space optical communications in atmospheric turbulence, J. Lightwave Technol., 27 (8) (2009) 967–973.

[27] A. P. Prudnikov, Y. A. Brychkov, and O. I. Marichev, Integral and Series, vol. 3: More Special Functions. Amsterdam: Gordon and Breach Science Publishers, 1986.

[28] E. Biglieri, J. Proakis and S. Shamai, Fading channels: information-theoretic and communications aspects, IEEE Trans. Inf. Theory, 44 (6) (1998) 2619-2692.